The EMBO Journal (2011) 30, 2501–2509 | © 2011 European Molecular Biology Organization | All Rights Reserved 0261-4189/11
www.embojournal.org

THE EMBO JOURNAL

APP heterozygosity averts memory deficit in knockin mice expressing the Danish dementia BRI2 mutant

Robert Tamayev[1], Shuji Matsuda[1], Luca Giliberto[1,4], Ottavio Arancio[2] and Luciano D'Adamio[1,3,*]

[1]Department of Microbiology and Immunology, Albert Einstein College of Medicine, Bronx, NY, USA, [2]Department of Pathology and Cell Biology, Taub Institute for Research on Alzheimer's Disease and the Aging Brain, Columbia University, New York, NY, USA and [3]National Research Council of Italy—Cellular Biology and Neurobiology Institute Via del Fosso del Fiorano, Roma, Italy

An autosomal dominant mutation in the *BRI2/ITM2B* gene causes familial Danish dementia (FDD). Analysis of FDD_{KI} mice, a mouse model of FDD genetically congruous to the human disease since they carry one mutant and one wild-type *Bri2/Itm2b* allele, has shown that the Danish mutation causes loss of Bri2 protein, synaptic plasticity and memory impairments. BRI2 is a physiological interactor of Aβ-precursor protein (APP), a gene associated with Alzheimer disease, which inhibits processing of APP. Here, we show that APP/Bri2 complexes are reduced in synaptic membranes of FDD_{KI} mice. Consequently, APP metabolites derived from processing of APP by β-, α- and γ-secretases are increased in Danish dementia mice. *APP* haplodeficiency prevents memory and synaptic dysfunctions, consistent with a role for APP metabolites in the pathogenesis of memory and synaptic deficits. This genetic suppression provides compelling evidence that APP and BRI2 functionally interact, and that the neurological effects of the Danish form of BRI2 only occur when sufficient levels of APP are supplied by two alleles. This evidence establishes a pathogenic sameness between familial Danish and Alzheimer's dementias.

The EMBO Journal (2011) **30,** 2501–2509. doi:10.1038/emboj.2011.161; Published online 17 May 2011
Subject Categories: neuroscience; molecular biology of disease
Keywords: APP; *BRI2/ITM2b*; familial Alzheimer disease; familial Danish dementia; mouse model

Introduction

Familial Danish dementia (FDD) and familial Alzheimer disease (FAD) are two genetically inherited autosomal dominant dementias. FDD is caused by a 10-nucleotide duplication preceding the stop codon of the *BRI2/ITM2B* gene (Vidal *et al*, 2000). In normal individuals, BRI2 is synthesized as an immature type-II membrane protein (imBRI2) that is cleaved at the C-terminus by a pro-protein convertase to produce mature BRI2 (mBRI2) and a 23-aa soluble C-terminal fragment (CTF) (Bri23) (Garringer *et al*, 2009). However, in FDD patients, a longer CTF, the ADan peptide (Vidal *et al*, 2000), is generated from the Danish mutant protein (BRI2-ADan), which has amyloidogenic properties. ADan forms amyloid angiopathy in the small blood vessels and capillaries of the cerebrum, choroid plexus, cerebellum, spinal cord and retina (Vidal *et al*, 2000). FDD patients also show diffuse brain atrophy, particularly in the cerebellum, cerebral cortex and white matter, as well as the presence of very thin and almost demyelinated cranial nerves; neurofibrillary tangles are the major histological finding in the hippocampus (Vidal *et al*, 2000).

FAD cases are caused by autosomal dominant mutations either in Aβ-precursor protein (*APP*) or in *Presenilins (PSEN1* and *PSEN2)* (St George-Hyslop and Petit, 2005), which are key components of a multi-molecular complex with γ-secretase activity (De Strooper, 2003). APP is normally sequentially cleaved by the β- and the γ-secretase. The γ-cut yields the Aβ peptide, consisting of two major species of 40 and 42 amino acids (Aβ40 and Aβ42, respectively, of which Aβ42 has amyloidogenic properties) (Wolfe, 2007) and an intracellular product termed the APP intracellular domain (AID or AICD) that regulates cell death (Passer *et al*, 2000) and gene transcription (Cao and Sudhof, 2001). However, the reported AID-dependent changes in gene expression have been questioned (Hebert *et al*, 2006; Giliberto *et al*, 2008). It is believed that FAD mutations in either *APP* or *PSEN1/2* favour the formation of the amyloidogenic Aβ42 peptide over the Aβ40 species.

The prevailing pathogenic theory of these human dementias, the 'amyloid cascade hypothesis' (Hardy and Selkoe, 2002), posits that the accumulation of neurotoxic amyloidogenic peptides triggers tauopathy, neurodegeneration, cognitive and behavioural changes. The amyloidogenic species are the ADan and Aβ42 peptides in FDD and FAD, respectively. Interestingly, in FDD Aβ co-deposits with ADan, mainly in vascular and perivascular amyloid lesions (Holton *et al*, 2002). We have recently proposed a different pathogenic model for FDD. This model asserts that memory loss in FDD is caused by loss of BRI2 function rather than the amyloidogenic ADan peptide (Tamayev *et al*, 2010b), and is supported by several lines of evidence: (1) FDD_{KI} mice present reduced mBri2 levels (similar to what is seen in FDD human brains); (2) the reduction in BRI2 is accompanied by significant synaptic and memory deficits; (3) these defects happen in the absence of obvious cerebral amyloidosis, tauopathy and reactive gliosis; (4) $Bri2^{+/-}$ mice present memory and synaptic

*Corresponding author. Department of Microbiology and Immunology, Albert Einstein College of Medicine, 1300 Morris Park Avenue, Chanin 514, Bronx, NY 10461, USA. Tel.: +1 718 430 3244; Fax: +1 718 430 8711; E-mail: luciano.dadamio@einstein.yu.edu
[4]Present address: The Litwin-Zucker Research Center for the Study of Alzheimer's Disease, The Feinstein Institute for Medical Research, North Shore—Long Island Jewish Health System, Manhasset, NY, USA

Received: 22 February 2011; accepted: 27 April 2011; published online: 17 May 2011

©2011 European Molecular Biology Organization

plasticity deficits; and (5) memory deficits of FDD_{KI} mice are prevented by expression of wild-type (WT) BRI2 in the forebrain (Giliberto *et al*, 2009; Tamayev *et al*, 2010a, b). The loss of function model is corroborated by the finding that transgenic models of FDD, that overexpress the Danish mutant BRI2 protein, present widespread cerebral amyloid angiopathy and parenchymal amyloid deposition of ADan peptide but do not show memory defects (Vidal *et al*, 2009; Coomaraswamy *et al*, 2010).

Compelling evidence indicates that BRI2 regulates processing of APP. BRI2 binds APP in the cellular compartments where APP is cleaved, that is the secretory pathway, plasma membrane and endocytic compartments (Matsuda *et al*, 2009). BRI2 binds to APP in the region that contains the cleavage sites and interferes with the docking of γ-secretase to C99 (Matsuda *et al*, 2008). In doing so, mBRI2 protects mAPP from processing. The evidence that mutations in *APP* and in genes that regulate APP processing, such as *Presenilins* and *BRI2*, cause dementias (Goate *et al*, 1990; Fotinopoulou *et al*, 2005; Matsuda *et al*, 2005, 2009; St George-Hyslop and Petit, 2005; Bertram and Tanzi, 2008; Garringer *et al*, 2009), emphasizes the relevance of APP processing to AD pathogenesis and prompted us to postulate that loss of BRI2 function in FDD leads to dementia via deregulation of APP processing. Here, we have investigated this hypothesis.

Results

APP/Bri2 complexes are reduced in synaptic membranes of FDD_{KI} mice

The mature form of BRI2 binds the mature form of APP *in vivo* (Matsuda *et al*, 2005, 2008, 2009). mBri2 is enriched in synaptic membranes and FDD_{KI} mice express low levels of mBri2 in brains and synapses, as compared with WT littermates (Tamayev *et al*, 2010b). Fractionation of synaptosomes showed that APP/Bri2 complexes are readily detected in synaptic fractions (Figure 1A). Immunoprecipitation with the α-BRI2 antibody and western blot with the α-APP antibody showed that APP/Bri2 complex was detectable both as crude synaptic fractions (Figure 1A and B) as well as purified synaptic membranes (Figure 1C). As FDD_{KI} mice have low levels of Bri2 in synapses, we measured APP/Bri2 complexes in synaptic fractions of FDD_{KI} mice. As could be predicted, FDD_{KI} mice have low levels of APP/Bri2 complexes in both crude (Figure 1B) and purified (Figure 1C and D) synaptic fractions. This finding is consistent with the hypothesis that the synaptic and memory dysfunctions of FDD_{KI} mice are due to reduced APP/Bri2 complexes.

APP processing is increased in FDD_{KI} mice

APP is cleaved by several proteases. Cleavage of APP by the β-secretase, which takes place prevalently in endocytic compartments, releases the APP ectodomain (sAPPβ) and a membrane-bound 99 amino acid-long fragment (C99). C99 is cleaved, with somewhat lax site specificity, by γ-secretase into Aβ and AID peptides. Alternatively, α-secretase cleaves APP, along the secretory pathway and on the plasma membrane, within the Aβ sequence to produce soluble APPα (sAPPα) and the membrane-bound C83 fragment (Wilquet and De Strooper, 2004; Marambaud and Robakis, 2005). BRI2 binds to APP and protects APP from α-, β- and γ-cleavage.

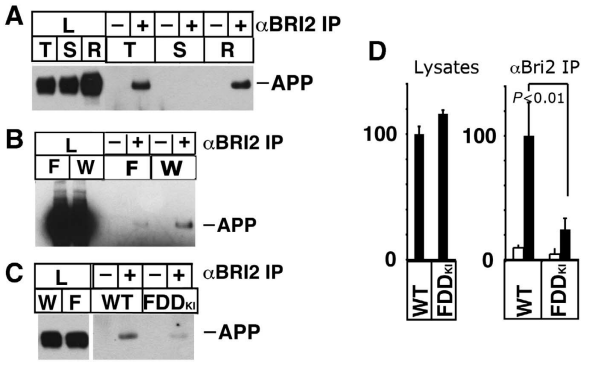

Figure 1 APP–Bri2 complexes are found in synaptic membrane preparations and are reduced in FDD_{KI} mice. (**A**) Crude synaptic membrane (P2) was extracted with buffers containing 0.5% Triton S-100 (T), 3% sarcosyl (S) and RIPA buffer (R). Each extract was precipitated with or without BRI2 antibody, and APP in lysates and precipitants were detected by 22C11. APP–Bri2 complexes are detected in T and R extracts but not S extracts. (**B**) P2 fraction was prepared from FDD_{KI} (F) and wild-type (W) mouse brains. P2 was extracted with the Hepes-Triton buffer, and the equal amounts of proteins were immunoprecipitated with rabbit polyclonal (−) or BRI2 antibody (+). APP was analysed as described above. (**C**) Immunoprecipitation (+) with α-BRI2 antibody from LP1 fractions shows that APP–Bri2 complexes are reduced in FDD_{KI} synaptic membranes as compared with WT. (**D**) Quantification by densitometric scans of blots stained with αAPP. The data represent the mean ± s.d. of triplicate experiments as in (**C**). The amounts of APP found in either the total lysates (left panel, lysates) or the Bri2 IPs (right panel, αBri2 IP) from the WT samples were assigned an arbitrary value of 100. The corresponding densitometric APP values of FDD_{KI} mice were expressed as a percentage of the WT mice value. The decrease in the amount of APP co-precipitated with Bri2 in FDD_{KI} mice is significant ($P<0.01$). The lysates loaded in the control lanes represent 25% of the lysates originally used for the IP lanes.

Thus, we tested whether the reduced levels of Bri2 and APP/Bri2 complexes modified APP processing in Danish dementia mice. Analysis of brain samples showed increased levels of sAPPα and sAPPβ in FDD_{KI} mice as compared with WT animals (Figure 2A–D, compare WT and FDD_{KI}-hets). To provide more definitive evidence on which APP metabolites are different, we also tested homozygote knockin mice because in these mice, the effects on APP processing could be more significant. As shown in Figure 2A–D in homozygous FDD_{KI} mice, both sAPPα and sAPPβ are statistically increased as compared with littermates. Aβ40 levels were, however, not significantly different between WT and either heterozygous (Tamayev *et al*, 2010b) or homozygous KI mice (not shown).

The increase in sAPPα and sAPPβ could be due to augmented production, due to the low levels in the inhibitor of processing Bri2, or to reduction in turnover, due to reduced degradation and/or export of sAPPα and sAPPβ from the CNS to peripheral tissues. To distinguish between these two possibilities, we prepared primary mouse dermal fibroblasts (MDFs) from WT and either heterozygous (Tamayev *et al*, 2010b) or homozygous FDD_{KI} mice. The cells were incubated with fresh media for 24 h and the levels of sAPPα were analysed. sAPPα was significantly more abundant in conditioned media from FDD_{KI} MDFs as compared with littermate controls (Figure 2E and F), supporting the conclusion that processing of APP is increased in FDD_{KI} mice.

Similarly, the equivalence in Aβ levels could indicate that γ-cleavage of C99 is not increased in FDD_{KI} mice.

 ©2011 European Molecular Biology Organization

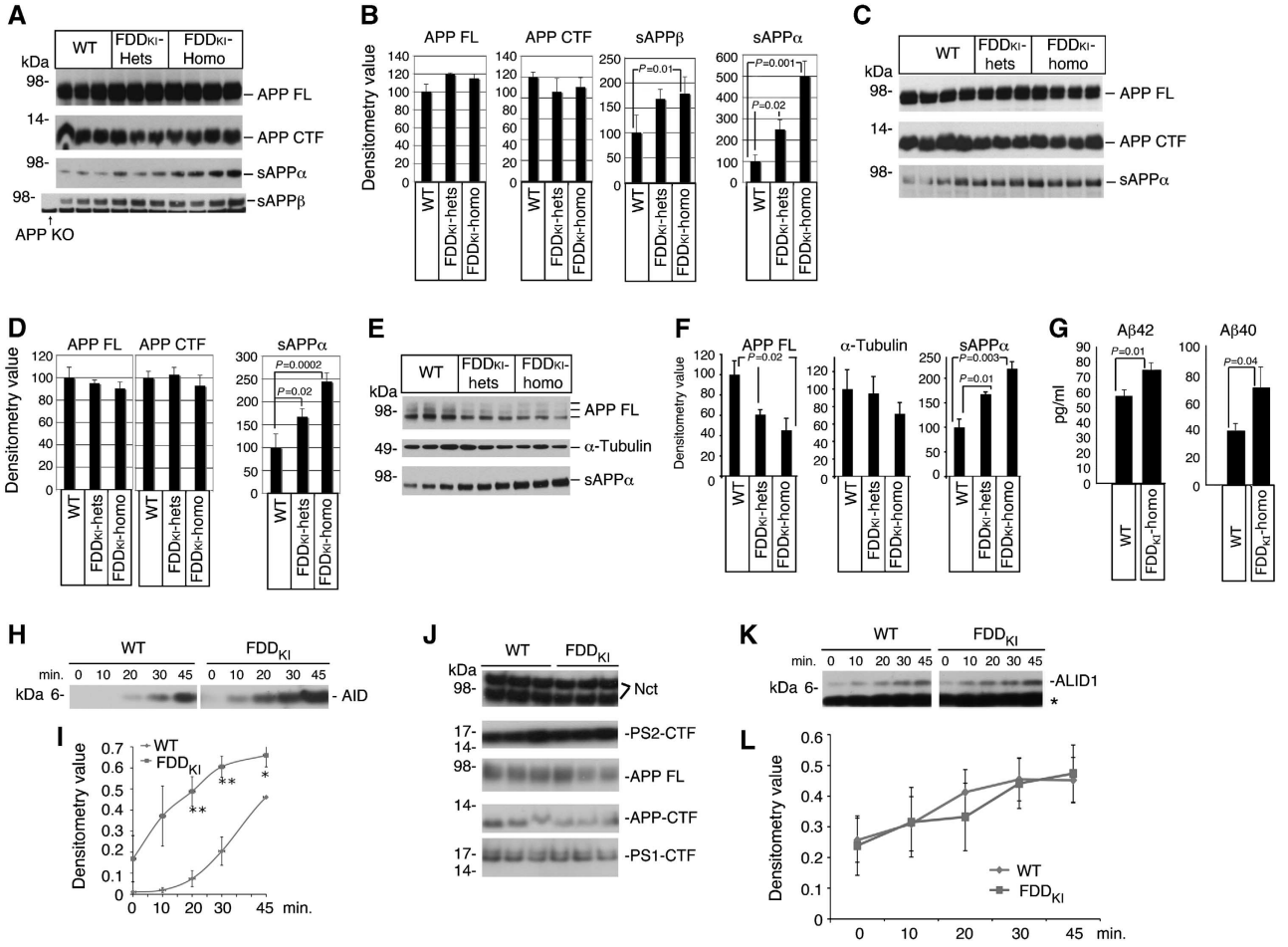

Figure 2 Increased APP processing in FDD_{KI} mice. (**A**) Western blot analysis of APP, sAPPα and sAPPβ levels in the brain of 11-month-old FDD_{KI} heterozygous ($n=3$, FDD_{KI}-hets), FDD_{KI} homozygous ($n=4$, FDD_{KI}-homo) and wild-type littermates ($n=3$, WT). (**B**) Quantitation of the data shown in (**A**). The values of sAPPα and sAPPβ were not adjusted for the variations in APP levels but were normalized according to the total brain proteins recovery. When compared with WT littermates, sAPPα was increased in a statistically significant manner in both FDD_{KI}-hets and FDD_{KI}-homo mice. (**C**) The experiment is similar to that shown in (**A**), except that the mice were 18 months old. (**D**) Quantization of the data shown in (**C**). The increase in sAPPα levels is statistically significant. (**E**) Western blot analysis of APP and α-tubulin in the cell lysates and of sAPPα in the supernatant of FDD_{KI}-hets, FDD_{KI}-homo and wild-type MDF cultures. It is worth noting that the levels of full-length APP decreased in knockin MDFs. This is consistent with an increase in cleavage of APP by α-secretase in these cells. The effect of the *Bri2* mutation on β-cleavage of APP is not reported since in these experimental settings the immunoblot with the α-sAPPβ antibody gave no signal. (**F**) Quantization of the data shown in (**E**). The increase in sAPPα levels is statistically significant. (**G**) Quantization of secreted human Aβ40 and Aβ42 in supernatants of *WT/APP–PS1* and FDD_{KI}-*homo/APP–PS1* cultures by ELISA. The data show that the PrP promoter drives expression of transgenic APP in fibroblasts and that the presence of the FDD mutation in Bri2 results in significant increase in both Aβ species. (**H**) An *in vitro* γ-secretase assay performed on LP1 fractions shows that γ-cleavage of APP is accelerated in FDD_{KI} mice. (**I**) Quantification of triplicate experiments as in (**H**). The increase in AID is significant ($^{*}P<0.05$; $^{**}P<0.01$). (**J**) Similar amounts of γ-secretase (determine by analysis of two of the four components, Nicastrin (Nct) and PS2/PS1 (PS2-Ctf and PS1-Ctf)), APP (both full-length (APP) and COOH-terminal fragments (APP-Ctf)) was present in the LP1 fractions used for the *in vitro* γ-secretase assay. (**K**) Western blot analysis of ALID1 (**APL**P1 **I**ntracellular **D**omain) in the *in vitro* γ-secretase assay performed on LP1 fractions. (**L**) Quantification of ALID1 in triplicate experiments as in (**K**) shows that γ-cleavage of APLP1 is comparable in FDD_{KI} and WT mice.

Alternatively, compensatory mechanisms, such as Aβ degradation or export of Aβ from the CNS to peripheral tissues, could maintain homoeostatic levels of Aβ in spite of increased production in FDD_{KI} mice. Measuring secreted Aβ in supernatant of cultured cells allows for a direct determination of Aβ production. In this experimental paradigm, others factors that may influence Aβ levels in the brain, such as Aβ catabolism and Aβ export from the central nervous system to the periphery are reduced or eliminated. Since endogenous murine Aβ levels are low and measurements tend to be noisy, we sought to employ a more robust measure of Aβ production. To this end, we crossed FDD_{KI} mice to APP695/PSEN1ΔE9 double transgenic mice (called here *APP–PS1*) expressing two familial Alzheimer's disease mutant genes (APP-Swedish and PSEN1ΔE9) (Savonenko *et al*, 2003). MDFs were isolated from an FDD_{KI}-homo/*APP–PS1* and a $Bri2^{wt/wt}$/*APP–PS1* mouse. Human Aβ40 and Aβ42 were detectable by ELISA in the culture supernatant of these MDFs. Importantly, we detected a significant elevation of secreted Aβ1-40 and Aβ1-42 in culture supernatant of FDD_{KI}-homo/*APP–PS1* MDFs (Figure 2G). These data are, again, reminiscent of the data obtained in $Bri2^{-/-}$ mice (Matsuda *et al*, 2008), indicating that the Danish mutation significantly impairs the inhibitory effect of BRI2 on the production of Aβ.

The increase in both Aβ40 and Aβ42 in the culture supernatant of homozygous FDD_{KI} MDFs expressing human

©2011 European Molecular Biology Organization

APP/PS1 suggests that γ-cleavage of C99 is also increased as a result of the FDD mutation in Bri2. To directly test γ-processing of APP-CTFs, we performed γ-secretase assays on synaptic membranes LP1 fractions. In this assay, γ-secretase activity is measured by monitoring endogenous AID (Sala Frigerio *et al*, 2009), which is produced when γ-secretase cleaves C99/C83 at the ε site (Weidemann *et al*, 2002; Sato *et al*, 2003). AID levels were increased in FDD_{KI} samples as compared with WT littermates (Figure 2H and I). Equal amounts of APP, APP-CTFs and γ-secretase were present in FDD_{KI} and WT preparations (Figure 2J). In addition, γ-cleavage of APLP1, a member of the *APP* gene family that is processed by γ-secretase as well (Scheinfeld *et al*, 2002; Sala Frigerio *et al*, 2009) but does not interact with BRI2 (Matsuda *et al*, 2008), was similar in both genotypes (Figure 2K and L). Altogether, these findings show that in FDD_{KI} mice, γ-cleavage of APP is augmented, while the levels and activity of the γ-secretase are not affected. This is consistent with the proposition that BRI2 reduces γ-cleavage of APP-CTFs by hampering docking of the γ-secretase and not via inhibition of the enzymatic activity of γ-secretase (Matsuda *et al*, 2008).

APP mediates synaptic defects in FDD_{KI} mice

In 1928, Ramon y Cajal predicted that dementia results from the weakening of synapses and some evidence supports a role for synaptic dysfunction underlying subtle memory changes in AD (Selkoe, 2002). Interestingly, FDD_{KI} mice have compromised long-term potentiation (LTP) (Tamayev *et al*, 2010b), a long-lasting form of synaptic plasticity that is thought to be associated with learning and memory. We tested whether the increase in APP metabolites due to loss of Bri2 function in FDD_{KI} mice underlies the synaptic and memory defects in FDD_{KI} mice. To this end, we crossed FDD_{KI} mice with heterozygous APP knockout ($APP^{+/-}$) mice and investigated synaptic transmission and plasticity using the Schaeffer collateral pathway in hippocampal slices from FDD_{KI} mice. Basal synaptic transmission (BST) was determined by measuring the slope of the field-excitatory-postsynaptic potential (fEPSP). We found no difference in BST in all four genotypes (WT, $APP^{+/-}$, FDD_{KI} and $FDD_{KI}/APP^{+/-}$) (Supplementary Figure S1). Paired-pulse facilitation (PPF) was also similar in all mice (Supplementary Figure S2), suggesting that no changes in Ca^{2+} mobilization or alterations in the probability of neurotransmitter release were driven by the mutation. As expected, LTP was reduced in FDD_{KI} mice compared with WT littermates (Figure 3). Strikingly, *APP* haplodeficiency prevented LTP impairments in FDD_{KI} mice (Figure 3).

APP mediates cognitive defects in FDD_{KI} mice

FDD_{KI} mice develop severe ageing-dependent memory deficits that first become measurable at ~5 months of age (Tamayev *et al*, 2010b). Thus, we tested whether reducing APP load would prevent memory loss in FDD_{KI} mice. In all, 11- to 14-month-old WT, $APP^{+/-}$, FDD_{KI}, $FDD_{KI}/APP^{+/-}$ mice were subjected to novel object recognition (NOR), a non-aversive task that relies on the mouse's natural exploratory behaviour. Open field studies showed that $APP^{+/-}$, FDD_{KI}, $FDD_{KI}/APP^{+/-}$ mice have no defects in habituation and locomotor behaviour, sedation, risk assessment and anxiety-like behaviour in novel environments

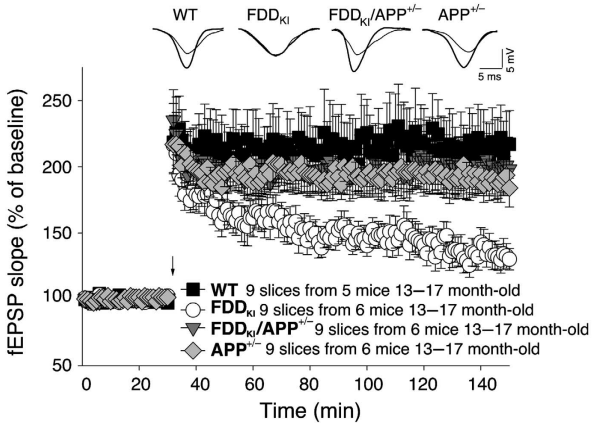

Figure 3 *APP* haplodeficiency prevents synaptic deficits of FDD_{KI} mice. Normal LTP in $FDD_{KI}/APP^{+/-}$ and $APP^{+/-}$ compared with WT mice by two-way ANOVA ($FDD_{KI}/APP^{+/-}$ versus WT mice: $F(1,16) = 0.569$; $P = 0.465$; $APP^{+/-}$ versus WT $F(1,16) = 0.557$; $P = 0.467$). Two-way ANOVA shows impaired LTP in FDD_{KI} mice when compared with WT ($F(1,16) = 6.745$; $P = 0.019$), to $FDD_{KI}/APP^{+/-}$ ($F(1,16) = 5.342$; $P = 0.035$) or to $APP^{+/-}$ mice littermates ($F(1,16) = 7.696$; $P = 0.014$).

(Supplementary Figure S3). During the training session, mice of all genotypes spent the same amount of time exploring the two identical objects (Figure 4A). The following day, when a novel object was introduced, FDD_{KI} spent the same amount of time exploring the two objects as if they were both novel to them, while the WT and $APP^{+/-}$ mice still spent more time exploring the novel object (Figure 4B). Notably, $FDD_{KI}/APP^{+/-}$ mice behaved like the WT mice and explored preferentially the novel object (Figure 4B). These data confirm that memory is impaired in FDD_{KI} mice upon ageing in an ethologically relevant, non-aversive behavioural context; remarkably, development of this deficit is fully prevented by *APP* haplodeficiency.

Next, we performed a spatial working memory test such as the radial-arm water maze (RAWM), which depends upon hippocampal function (Diamond *et al*, 1999) and tests short-term memory, a type of memory that is affected at early stages of AD. Mice were required to learn and memorize the location of a hidden platform in one of the arms of a maze with respect to spatial cues. WT and $APP^{+/-}$ mice were able to acquire (A) and retain (R) memory of the task. FDD_{KI} mice showed severe abnormalities during both acquisition and retention of the task (Figure 5), confirming that FDD_{KI} mice have severe impairment in short-term spatial memory for platform location during both acquisition and retention of the task. This defect was due to a deficit in memory *per se* and not to deficits in vision, motor coordination or motivation because testing with the visible platform showed no difference in the time needed to find the platform and swimming speed between the FDD_{KI} and WT mice (Supplementary Figures S4 and S5). Once again, halving APP expression prevented the development of short-term spatial memory in FDD_{KI} mice (Figure 5). Taken together, these findings provide compelling genetic evidence that APP and BRI2 functionally interact, and that the synaptic and memory deficiencies due to loss of Bri2 function only occurs when sufficient levels of APP are supplied by two alleles.

©2011 European Molecular Biology Organization

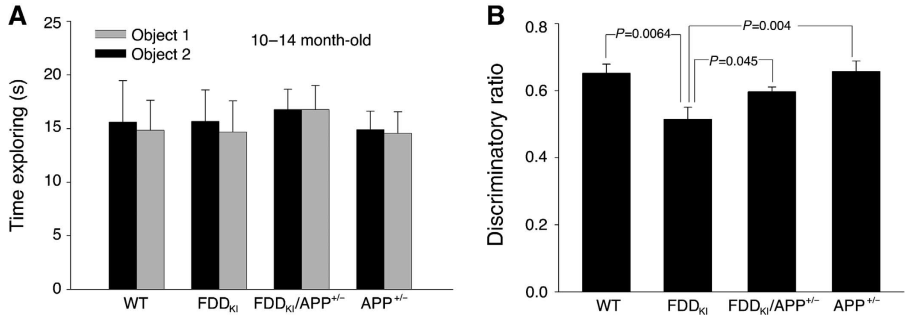

Figure 4 *APP* haplodeficiency prevents the Novel object recognition deficit of FDD_{KI} mice. (**A**) All four genotypes (WT, $APP^{+/-}$, FDD_{KI} and $FDD_{KI}/APP^{+/-}$) mice spent similar amounts of time exploring the two identical objects on day 1. (**B**) WT, $APP^{+/-}$ and $FDD_{KI}/APP^{+/-}$ mice performed similarly in NOR tests (WT versus $APP^{+/-}$, $P=0.93$; WT versus $FDD_{KI}/APP^{+/-}$, $P=0.079$), showing that APP haplodeficiency prevents the novel object recognition deficit of FDD_{KI} mice (FDD_{KI} versus $FDD_{KI}/APP^{+/-}$, $P=0.045$).

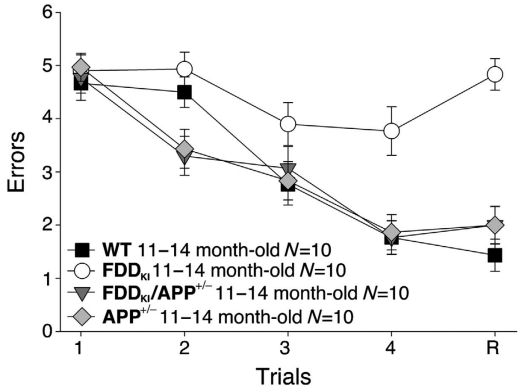

Figure 5 *APP* haplodeficiency prevents the RAWM deficits of FDD_{KI} mice. In RAWM testing, $APP^{+/-}$ and $FDD_{KI}/APP^{+/-}$ mice made the same number of errors as WT mice. FDD_{KI} mice made significantly more errors at A3 (versus $FDD_{KI}/APP^{+/-}$ $P<0.05$; versus WT $P<0.05$), A4 (versus $APP^{+/-}$ $P<0.001$; versus $FDD_{KI}/APP^{+/-}$ $P<0.001$; versus WT, $P<0.001$) and R (versus $APP^{+/-}$ $P<0.0001$; versus $FDD_{KI}/APP^{+/-}$ $P<0.0001$; versus WT, $P<0.0001$). Thus, *APP* haplodeficiency prevents the insurgence of working memory deficits in FDD_{KI} mice.

Discussion

Here, we have investigated the mechanisms by which loss of BRI2 function in FDD, alternative to the amyloid model (Figure 6A and B), leads to synaptic plasticity deficits and memory impairment. Since BRI2 is a physiological regulator of APP processing, we have tested whether APP processing is altered in FDD_{KI} mice and whether these alterations lead to synaptic and memory deficits. We show an ~75% reduction in mBri2/mAPP complexes in brains and in synaptic membranes of FDD_{KI} mice, which is expected given the lower levels of Bri2 proteins in these mice (Tamayev *et al*, 2010b). Consistent with the proposed function of mBRI2, FDD_{KI} mice show increased processing of APP. Strikingly, *APP* haplodeficiency prevents memory and synaptic dysfunctions in FDD_{KI} mice, supporting the claim that Danish dementia is mediated, like FAD, through toxic APP products. In contrast with the amyloid cascade hypothesis (Hardy and Selkoe, 2002), our data present no evidence supporting a role for ADan in synaptic plasticity and memory deficits. Transgenic mouse models of FDD reproduce amyloidosis (Vidal *et al*, 2009; Coomaraswamy *et al*, 2010). These mice are genetically non-congruous with the human diseases since the mutant transgene is expressed in an artificial quantitative-spatio-temporal manner, and do not replicate loss of function, given the persistence of the two endogenous WT mouse alleles. On the contrary, FDD transgenic mice express elevated brain levels of mBRI2 (Coomaraswamy *et al*, 2010), which is opposite to what was observed in FDD_{KI} mice and, more importantly, in FDD human cases (Tamayev *et al*, 2010b). Despite the considerable amyloidosis, memory loss has not been described in FDD transgenic mice (Vidal *et al*, 2009; Coomaraswamy *et al*, 2010). It is also worth noting that in human FDD cases, ADan and Aβ42 co-deposits in a subset of amyloid plaques (Vidal *et al*, 2000). However, the expression of the FDD transgene in human *APP* transgenic mice not only does not lead to formation of ADan/Aβ42 mixed plaques, but in contradiction causes an extensive reduction in Aβ amyloid plaques (Coomaraswamy *et al*, 2010). This is consistent with the hypothesis that an increase in mBRI2 levels reduces processing of APP (Matsuda *et al*, 2008). Thus, the lack of co-deposition of human ADan and Aβ42 and the inhibitory effect on Aβ42 in FDD transgenic mice (Coomaraswamy *et al*, 2010) further stresses the incongruence of the transgenic model with the human disease.

The ADan peptide may start other clinical symptoms that are present in Danish dementia patients, such as cataracts, deafness and progressive ataxia, but are not replicated in FDD_{KI} mice. In addition, in the late phase of the disease, accumulation of oligomeric ADan, which is toxic to neuronal cell lines (Gibson *et al*, 2004), may cause neuronal degeneration and neuronal loss, which are associated with FDD but are not obviously detectable in FDD_{KI} mice. The neurotoxicity of oligomeric ADan may also be limited to *in vitro* systems since ADan amyloidosis does not lead to neuronal loss in transgenic mice (Vidal *et al*, 2009; Coomaraswamy *et al*, 2010).

What is the molecular nature of this (these) toxic product(s)? The obvious candidate is Aβ42, which is widely implicated in AD pathogenesis. However, we are technically unable to reproducibly measure murine Aβ42 in mouse brains, and quantification of the shorter but more abundant Aβ40 species showed no changes between FDD_{KI} and WT mouse brains (Tamayev *et al*, 2010b). However, primary cells derived from mice carrying the Danish mutation on both *Bri2* alleles, produce higher levels of both Aβ42 and Aβ40. Thus, it is possible that in FDD_{KI} mice there is a pathological increase in Aβ42 and/or in Aβ42 over Aβ40, like seen in FAD cases

©2011 European Molecular Biology Organization

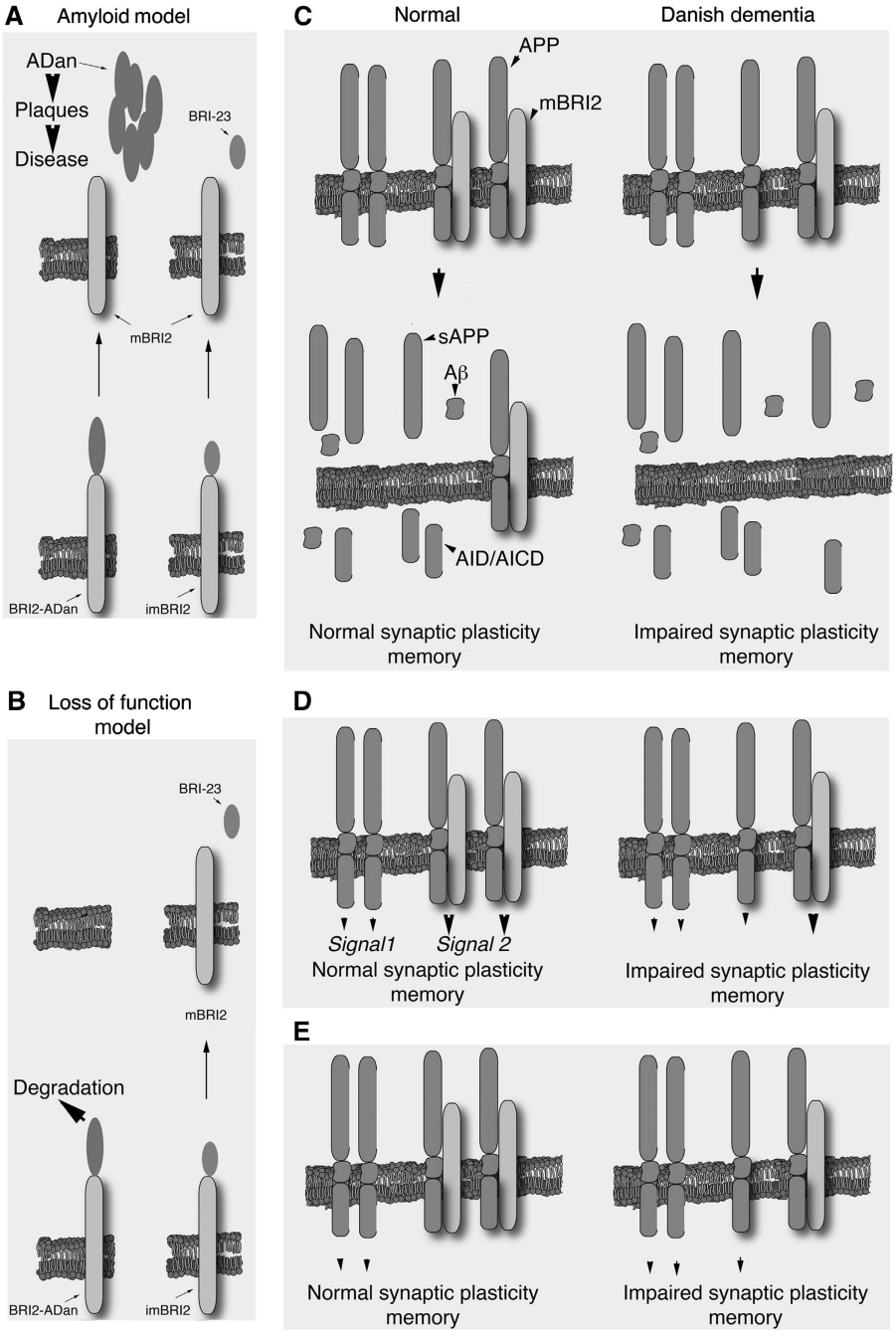

Figure 6 Models depicting the mechanisms by which APP leads to memory deficits in FDD. (**A**) Immature WT BRI2 (imBRI2) and BRI2-ADan are cleaved by a convertases to mBRI2. The cleavage releases a C-terminal 23 amino-acid peptide (Bri23) from imBRI2, and the ADan peptide from BRI2-ADan. The current model of FDD pathogenesis asserts that the amyloid lesion causes the disease (Amyloid model). (**B**) The Danish mutation targets BRI2 for degradation (unpublished observations). This results in a loss of mature BRI2 protein that cause synaptic and memory deficits (loss of function model). (**C**) In this model, synaptic and memory deficits in FDD are caused by the increased production of one or more toxic APP-derived metabolites due to loss of inhibitory function of APP processing by BRI2. (**D**) Alternatively, membrane-bound BRI2, APP and APP/BRI2 complexes could regulate distinct signalling pathways (indicated as signal-1, -2 and -3, respectively). In FDD, the reduction of BRI2 levels result in a 'signalling unbalance' leading to synaptic and memory dysfunction. (**E**) Finally, APP and BRI2 may signal only when not bound to each other. The loss of BRI2 in FDD would decrease the BRI2 signal and increase the APP signal, thereby causing memory and synaptic impairments.

due to *PSEN1/2* mutations. Increases in Aβ42 and/or Aβ42 to Aβ40 ratio are considered pathogenic since they would favour aggregation of Aβ42. It is also possible that toxic forms of Aβ may, transiently perhaps, increase in pathological niches and escape detection when sampling the whole brain. Besides Aβ, various APP-derived fragments, such as AID/AICD (Passer *et al*, 2000; Giliberto *et al*, 2008; Ghosal *et al*, 2009), C31 (Galvan *et al*, 2006), Jcasp (Madeira *et al*, 2005), sAPPβ (Nikolaev *et al*, 2009) have been implicated in neurodegenerative processes. These APP-derived metabolites could also cooperate in precipitating synaptic dysfunction and memory loss in human dementia cases (Figure 6C).

 ©2011 European Molecular Biology Organization

Although the most straightforward interpretation of our data is that fragments derived from APP processing cause memory loss in FDD, it is possible that APP and BRI2 protein, as well as the APP/BRI2 complex, have a pathogenic role. Membrane-bound APP, BRI2 and APP/BRI2 complexes could deliver distinct signals (signal 1, signal 2 and signal 3) that are important for normal synaptic transmission and memory formation/consolidation. In FDD, an augmentation of signal 2 and a reduction of signals 1 and 3 could generate a 'signalling unbalance' that leads to memory deficits (Figure 6D). Also, membrane-bound APP and/or BRI2 could trigger signalling pathways that are necessary for normal memory functions, and that these signals are inhibited when APP and BRI2 are bound. In FDD, excessive APP-mediated signalling over BRI2-mediated signalling could cause alterations of normal synaptic functions and memory impairments (Figure 6E). In all cases, reducing APP load would reconstitute normal signalling.

In conclusion, genetic suppression of cognitive deficits by *APP* haplodeficiency shows that FDD pathogenesis may be attributable to APP and/or toxic APP products. This mechanism presents strong analogies with the pathogenesis of classical familial Alzheimer cases, where *APP* itself or genes that, like *BRI2*, regulate APP processing (i.e. *PSEN1/2*) are mutated. Overall, our data suggest that the FDD_{KI} mouse is an excellent model to test both the pathogenicity of APP and/or proteolytic APP products, as well as disease-modifying therapeutic intervention strategies for resulting dementias.

Materials and methods

Mouse transgenic lines

B6C3-Tg (APPswe, PSEN1ΔE9) 85Dbo/J mice were purchased from The Jackson Laboratory (Savonenko *et al*, 2003). This is a double transgenic mouse expressing a chimeric mouse/human amyloid precursor protein (Mo/HuAPP695swe) and a mutant human PSEN1 (PSEN1ΔE9) under the control of the Syrian hamster prion promoter. Both mutations are associated with early onset AD. These mice secrete human Aβ peptides.

Mouse handling

Mice were handled according to the Ethical Guidelines for Treatment of Laboratory Animals of Albert Einstein College of Medicine. The procedures were described and approved in animal protocol number 200404.

Mouse brain preparations for western blot

FDD_{KI} and $APP^{+/-}$ mice are on a C57BL/6J background. Mice were handled according to the Ethical Guidelines for Treatment of Laboratory Animals of Einstein. Brain samples were prepared by homogenizing brains (w/v = 10 mg tissue/100 ml buffer) in Hepes-sucrose buffer (20 mM Hepes/NaOH pH 7.4, 1 mM EDTA, 1 mM EGTA, 0.25 M sucrose) supplemented with protease and phosphatase inhibitors (PI and PhI). The postnuclear supernatant (PNS) was prepared by precipitating the nuclei and debris by centrifuging the homogenates at 1000 *g* for 10 min. In all, 20 μg of each PNS were loaded on SDS–PAGE. To prepare mouse brain membranes and soluble fraction PNS was cleared by centrifuging at 100 kg for 45 min. The precipitated membranes were suspended in Hepes-sucrose buffer and equal amount of proteins were used for WB. The supernatants (soluble fractions) were used for sAPPα and sAPPβ western blot.

MDFs and Aβ ELISA

To culture MDFs, skin was removed from mouse tails, soaked in 70% ethanol, washed in PBS, diced into small pieces and incubated at 37°C overnight in CO_2 incubator in DMEM containing 20% FBS, supplemented with penicillin/streptomycin and 1.6 mg/ml collagenase II. On the next day, clumps were removed by passing through a nylon mesh, and the material was centrifuged at 1000 r.p.m. for 5 min to collect the cells. The collected cells were maintained in DMEM containing 20% FBS and penicillin/streptomycin. To measure Aβ production, the cells were conditioned for 24 h, and Aβ in the medium was measured using the ELISA kit for Aβ40 and Aβ42 (IBL 17713 and 17711, respectively).

Antibodies

The following antibodies were used: α-APP (22C11, Chemicon MAB348); α-sAPPα (IBL 11088); α-sAPPβ (IBL 18957); α-APP CTFs (α-APPct Invitrogen/Zymed 36-6900); α-calnexin (Stressgen SPA-865); α-tubulin (Sigma DM1A); α-GM130 (Sigma G7295); α-PS1-Ctf (Calbiochem 529592); α-Nct (Cell Signaling 5665); α-PS2-Ctf (Calbiochem 529594); BRI2 antibody (recognizing amino acids 7–21 of human BRI2) was a generous gift from Dr Haruhiko Akiyama (Akiyama *et al*, 2004). Secondary antibodies conjugated with horseradish peroxidase are from Southern Biotechnology.

Synaptosomes preparations

Mouse brain was homogenized in H buffer (5 mM Hepes/NaOH pH 7.4, 1 mM EDTA, 1 mM EGTA, 0.32 M sucrose, plus PI/PhI at 10% (w/v)) and centrifuged at 800 *g* for 10 min. The supernatant (S1) was separated to supernatant (S2) and pellet (P2) by spinning at 9200 *g* for 15 min. P2 was lysed on ice for 30 min in H buffer containing 35.6 mM sucrose. The lysed P2 was separated to supernatant (LS1) and pellet (LP1) by spinning at 25 000 *g* for 20 min. Synaptosomes fractions represent: P2, crude synaptosomal fraction; LP1, synaptic membrane fraction.

APP/Bri2 complexes isolation and quantification

The crude synaptic membrane was extracted with the Hepes-Triton buffer (T: 20 mM Hepes/NaOH, 1 mM EDTA, 1 mM EGTA, 150 mM NaCl, 0.5% Triton X-100), the Hepes-sarcosyl buffer (S: 3% sarcosyl instead of 0.5% Triton X-100) and the RIPA buffer (R: 0.5% sodium deoxycholate and 0.1% SDS was added to the Hepes-Triton buffer) and cleared by spinning at 20 000 *g* for 10 min. Equal amounts of each cleared extract were precleared with protein A beads. Precleared extracts were mixed with rabbit polyclonal (−) or α-BRI2 (+) antibody, and proteins bound to the antibodies were precipitated with protein A beads. The beads were washed in the corresponding buffers, and boiled in 2× SDS buffer. The APP in lysates and precipitants were detected by western blot.

P2 was prepared as described above. The P2 fraction was layered on top of a discontinuous sucrose gradient (5 mM Hepes/NaOH pH 7.4, 1 mM EDTA, 1 mM EGTA containing 1.2 M (3 ml), 1.0 M (3 ml) and 0.8 M (4 ml) sucrose). After the banding at 150 000 *g* for 2 h, the band between 1.2 and 1.0 M sucrose was collected as synaptic plasma membrane (SPM). SPM was diluted with the Hepes buffer (5 mM Hepes/NaOH pH 7.4, 1 mM EDTA) and precipitated by spinning at 150 000 *g* for 2 h. The precipitated SPM was extracted with the Hepes-Triton buffer, and cleared by spinning at 100 000 *g* for 45 min. The pellet was further extracted with the RIPA buffer, and cleared as above. The Hepes-Triton buffer extract (T) and the RIPA buffer extract (R) were immunoprecipitated with rabbit polyclonal antibody (−) or BRI2 antibody (+), and APP was analysed as described above.

The in vitro γ-secretase assay

The *in vitro* γ-secretase assay was performed on LP1 fractions as described (Sala Frigerio *et al*, 2009). Briefly, synaptosomes were incubated at 37° for 0, 10, 20, 30 and 45 min, and then spun at 150 000 *g* for 75 min. The supernatants and pellets were run separately, and blotted for AICD, Nicastrin, PS2-Ctf, PS1-Ctf, full-length APP and APP-Ctf.

Image scanning and analysis

WB and radiography images were scanned with Epson perfection 3200 Photo scanner and were analysed with NIH ImageJ software. All quantified data represent an average of at least triplicate samples. Error bars represent s.d. Statistical significance was determined by Student's *t*-test and a $P<0.05$ was considered significant.

Electrophysiological and behaviour

The animals used for these studies were backcrossed to C57Bl6/J mice for at least 14 generations. Only male mice were used to avoid variations due to hormonal fluctuations during the menstrual

©2011 European Molecular Biology Organization

female cycle, which influence severely behavioural and electrophysiological tests.

Electrophysiology

Electrophysiology experiments were performed as previously described (Puzzo *et al*, 2008). Transverse hippocampal slices (400 μm) were transferred to a recording chamber where they were maintained at 29°C and perfused with artificial cerebrospinal fluid (ACSF) continuously bubbled with 95% O_2 and 5% CO_2. The ACSF composition in mM was: 124 NaCl, 4.4 KCl, 1 Na_2HPO_4, 25 $NaHCO_3$, 2 $CaCl_2$, 2 $MgSO_4$ and 10 glucose. CA1 fEPSPs were recorded by placing both the stimulating and the recording electrodes in CA1 stratum radiatum (Tomidokoro *et al*, 2005). BST was estimated by measuring the slope of the fEPSP at different stimulus intensities. PPF was tested using 10 interstimulus intervals (10, 20, 30, 40, 50, 100, 200, 300, 500 and 1000 ms) and defined as the second fEPSP slope expressed as a percentage of the first. For LTP experiments, a 30-min baseline was recorded every minute at an intensity that evoked a response ~35% of the maximum evoked response. LTP was induced using a θ-burst stimulation (four pulses at 100 Hz, with bursts repeated at 5 Hz and each tetanus including one 10-burst train). Responses were recorded for 2 h after tetanization and plotted as percentage of baseline fEPSP slope.

Spatial working memory

The task studied with the RAWM test has been described previously (Trinchese *et al*, 2004). The scores for each mouse on the last 3 days of testing were averaged and used for statistical analysis. Briefly, a six-armed maze was placed into white tank filled with water (24–25°C) and made opaque by the addition of non-toxic white paint. Spatial cues were presented on the walls of the testing room. At the end of one of the arms was positioned a clear 10 cm submerged platform that remained in the same location for every trial in 1 day but was moved approximately randomly from day to day. On each trial, the mouse started the task from a different randomly chosen arm. Each trial lasted 1 min, and errors were counted each time the mouse entered the wrong arm or needed >10 s to reach the platform. After each error, the mouse was pulled back to its starting position. After four consecutive acquisition trials, the mouse was placed in its home cage for 30 min, then returned to the maze and administered a fifth retention trial.

Visible platform testing

Visible platform training to test visual and motor deficits was performed in the same pool as in the RAWM; however, the arms of the maze were removed. The platform was marked with a black flag and positioned randomly from trial to trial. Time to reach the platform and speed were recorded with a video tracking system (HVS 2020; HVS Image).

Open field and NOR

After 30 min to acclimate to the testing room, each mouse was placed into a $40 \times 40\,cm^2$ open field chamber with 2 ft high opaque walls. Each mouse was allowed to habituate to the normal open field box for 10 min, and repeated again 24 h later, in which the video tracking system (HVS 2020; HVS Image) quantifies the number of entries into and time spent in the centre of the locomotor arena. NOR was performed as previously described (Bevins and Besheer, 2006). Results were recorded as an object discrimination ratio, which is calculated by dividing the time the mice spent exploring the novel object, divided by the total amount of time exploring the two objects.

Statistical analysis

All data are shown as mean ± s.e.m. Experiments were performed in blind. Statistical tests included two-way ANOVA for repeated measures and *t*-test when appropriate.

Supplementary data

Supplementary data are available at *The EMBO Journal* Online (http://www.embojournal.org).

Acknowledgements

This work was supported by grants from the Alzheimer's Association (IIRG-09-129984 to LD), the National Institutes of Health (NIH; R01AG033007 to LD and R01NS049442 to OA) and the Edward N & Della L Thome Memorial Foundation grant (to LD).

Author contributions: RT, SM and LG performed experiments and contributed to figures; OA provided assistance with electrophysiological and behavioural experiments and contributed to data discussion; LD designed the research, performed experiments, contributed to figures and wrote the paper.

Conflict of interest

LG and LD are inventors of an AECOM patent on the FDD mice. The mice discussed in this paper (BRI2-ADan knockin mice) are patent-pending. The assign is the Albert Einstein College of Medicine. The Albert Einstein College of Medicine has licensed the patent to a Biotech company (Remegenix) of which Dr D'Adamio is a co-founder.

References

Akiyama H, Kondo H, Arai T, Ikeda K, Kato M, Iseki E, Schwab C, McGeer PL (2004) Expression of BRI, the normal precursor of the amyloid protein of familial British dementia, in human brain. *Acta Neuropathol (Berl)* **107:** 53–58

Bertram L, Tanzi RE (2008) Thirty years of Alzheimer's disease genetics: the implications of systematic meta-analyses. *Nat Rev Neurosci* **9:** 768–778

Bevins RA, Besheer J (2006) Object recognition in rats and mice: a one-trial non-matching-to-sample learning task to study 'recognition memory'. *Nat Protoc* **1:** 1306–1311

Cao X, Sudhof TC (2001) A transcriptionally [correction of transcriptively] active complex of APP with Fe65 and histone acetyltransferase Tip60. *Science* **293:** 115–120

Coomaraswamy J, Kilger E, Wolfing H, Schafer C, Kaeser SA, Wegenast-Braun BM, Hefendehl JK, Wolburg H, Mazzella M, Ghiso J, Goedert M, Akiyama H, Garcia-Sierra F, Wolfer DP, Mathews PM, Jucker M (2010) Modeling familial Danish dementia in mice supports the concept of the amyloid hypothesis of Alzheimer's disease. *Proc Natl Acad Sci USA* **107:** 7969–7974

De Strooper B (2003) Aph-1, Pen-2, and Nicastrin with Presenilin generate an active gamma-secretase complex. *Neuron* **38:** 9–12

Diamond DM, Park CR, Heman KL, Rose GM (1999) Exposing rats to a predator impairs spatial working memory in the radial arm water maze. *Hippocampus* **9:** 542–552

Fotinopoulou A, Tsachaki M, Vlavaki M, Poulopoulos A, Rostagno A, Frangione B, Ghiso J, Efthimiopoulos S (2005) BRI2 interacts with amyloid precursor protein (APP) and regulates amyloid beta (Abeta) production. *J Biol Chem* **280:** 30768–30772

Galvan V, Gorostiza OF, Banwait S, Ataie M, Logvinova AV, Sitaraman S, Carlson E, Sagi SA, Chevallier N, Jin K, Greenberg DA, Bredesen DE (2006) Reversal of Alzheimer's-like pathology and behavior in human APP transgenic mice by mutation of Asp664. *Proc Natl Acad Sci USA* **103:** 7130–7135

Garringer HJ, Murrell J, D'Adamio L, Ghetti B, Vidal R (2009) Modeling familial British and Danish dementia. *Brain Struct Funct* **214:** 235–244

Ghosal K, Vogt DL, Liang M, Shen Y, Lamb BT, Pimplikar SW (2009) Alzheimer's disease-like pathological features in transgenic mice expressing the APP intracellular domain. *Proc Natl Acad Sci USA* **106:** 18367–18372

Gibson G, Gunasekera N, Lee M, Lelyveld V, El-Agnaf OM, Wright A, Austen B (2004) Oligomerization and neurotoxicity of the amyloid ADan peptide implicated in familial Danish dementia. *J Neurochem* **88:** 281–290

Giliberto L, Matsuda S, Vidal R, D'Adamio L (2009) Generation and initial characterization of FDD knock in mice. *PLoS One* **4:** e7900

Giliberto L, Zhou D, Weldon R, Tamagno E, De Luca P, Tabaton M, D'Adamio L (2008) Evidence that the Amyloid beta precursor protein-intracellular domain lowers the stress threshold of neurons

 ©2011 European Molecular Biology Organization

and has a 'regulated' transcriptional role. *Mol Neurodegener* **3:** 12

Goate AM, Hardy JA, Owen MJ, Haynes A, James L, Farrall M, Mullan MJ, Roques P, Rossor MN (1990) Genetics of Alzheimer's disease. *Adv Neurol* **51:** 197–198

Hardy J, Selkoe DJ (2002) The amyloid hypothesis of Alzheimer's disease: progress and problems on the road to therapeutics. *Science* **297:** 353–356

Hebert SS, Serneels L, Tolia A, Craessaerts K, Derks C, Filippov MA, Muller U, De Strooper B (2006) Regulated intramembrane proteolysis of amyloid precursor protein and regulation of expression of putative target genes. *EMBO Rep* **7:** 739–745

Holton JL, Lashley T, Ghiso J, Braendgaard H, Vidal R, Guerin CJ, Gibb G, Hanger DP, Rostagno A, Anderton BH, Strand C, Ayling H, Plant G, Frangione B, Bojsen-Moller M, Revesz T (2002) Familial Danish dementia: a novel form of cerebral amyloidosis associated with deposition of both amyloid-Dan and amyloid-beta. *J Neuropathol Exp Neurol* **61:** 254–267

Madeira A, Pommet JM, Prochiantz A, Allinquant B (2005) SET protein (TAF1beta, I2PP2A) is involved in neuronal apoptosis induced by an amyloid precursor protein cytoplasmic subdomain. *FASEB J* **19:** 1905–1907

Marambaud P, Robakis NK (2005) Genetic and molecular aspects of Alzheimer's disease shed light on new mechanisms of transcriptional regulation. *Genes Brain Behav* **4:** 134–146

Matsuda S, Giliberto L, Matsuda Y, Davies P, McGowan E, Pickford F, Ghiso J, Frangione B, D'Adamio L (2005) The familial dementia BRI2 gene binds the Alzheimer gene amyloid-beta precursor protein and inhibits amyloid-beta production. *J Biol Chem* **280:** 28912–28916

Matsuda S, Giliberto L, Matsuda Y, McGowan EM, D'Adamio L (2008) BRI2 inhibits amyloid beta-peptide precursor protein processing by interfering with the docking of secretases to the substrate. *J Neurosci* **28:** 8668–8676

Matsuda S, Matsuda Y, Snapp EL, D'Adamio L (2009) Maturation of BRI2 generates a specific inhibitor that reduces APP processing at the plasma membrane and in endocytic vesicles. *Neurobiol Aging* (advance online publication)

Nikolaev A, McLaughlin T, O'Leary DD, Tessier-Lavigne M (2009) APP binds DR6 to trigger axon pruning and neuron death via distinct caspases. *Nature* **457:** 981–989

Passer B, Pellegrini L, Russo C, Siegel RM, Lenardo MJ, Schettini G, Bachmann M, Tabaton M, D'Adamio L (2000) Generation of an apoptotic intracellular peptide by gamma-secretase cleavage of Alzheimer's amyloid beta protein precursor. *J Alzheimers Dis* **2:** 289–301

Puzzo D, Privitera L, Leznik E, Fa M, Staniszewski A, Palmeri A, Arancio O (2008) Picomolar amyloid-beta positively modulates synaptic plasticity and memory in hippocampus. *J Neurosci* **28:** 14537–14545

Sala Frigerio C, Kukar TL, Fauq A, Engel PC, Golde TE, Walsh DM (2009) An NSAID-like compound, FT-9, preferentially inhibits gamma-secretase cleavage of the amyloid precursor protein compared to its effect on amyloid precursor-like protein 1. *Biochemistry* **48:** 10894–10904

Sato T, Dohmae N, Qi Y, Kakuda N, Misonou H, Mitsumori R, Maruyama H, Koo EH, Haass C, Takio K, Morishima-Kawashima M, Ishiura S, Ihara Y (2003) Potential link between amyloid beta-protein 42 and C-terminal fragment gamma 49-99 of beta-amyloid precursor protein. *J Biol Chem* **278:** 24294–24301

Savonenko AV, Xu GM, Price DL, Borchelt DR, Markowska AL (2003) Normal cognitive behavior in two distinct congenic lines of transgenic mice hyperexpressing mutant APP SWE. *Neurobiol Dis* **12:** 194–211

Scheinfeld MH, Ghersi E, Laky K, Fowlkes BJ, D'Adamio L (2002) Processing of beta-amyloid precursor-like protein-1 and -2 by gamma-secretase regulates transcription. *J Biol Chem* **277:** 44195–44201

Selkoe DJ (2002) Alzheimer's disease is a synaptic failure. *Science* **298:** 789–791

St George-Hyslop PH, Petit A (2005) Molecular biology and genetics of Alzheimer's disease. *C R Biol* **328:** 119–130

Tamayev R, Giliberto L, Li W, d'Abramo C, Arancio O, Vidal R, D'Adamio L (2010a) Memory deficits due to familial British dementia BRI2 mutation are caused by loss of BRI2 function rather than amyloidosis. *J Neurosci* **30:** 14915–14924

Tamayev R, Matsuda S, Fa M, Arancio O, D'Adamio L (2010b) Danish dementia mice suggest that loss of function and not the amyloid cascade causes synaptic plasticity and memory deficits. *Proc Natl Acad Sci USA* **107:** 20822–20827

Tomidokoro Y, Lashley T, Rostagno A, Neubert TA, Bojsen-Moller M, Braendgaard H, Plant G, Holton J, Frangione B, Revesz T, Ghiso J (2005) Familial Danish dementia: co-existence of Danish and Alzheimer amyloid subunits (ADan AND A{beta}) in the absence of compact. *J Biol Chem* **280:** 36883–36894

Trinchese F, Liu S, Battaglia F, Walter S, Mathews PM, Arancio O (2004) Progressive age-related development of Alzheimer-like pathology in APP/PS1 mice. *Ann Neurol* **55:** 801–814

Vidal R, Barbeito AG, Miravalle L, Ghetti B (2009) Cerebral amyloid angiopathy and parenchymal amyloid deposition in transgenic mice expressing the Danish mutant form of human BRI2. *Brain Pathol* **19:** 58–68

Vidal R, Revesz T, Rostagno A, Kim E, Holton JL, Bek T, Bojsen-Moller M, Braendgaard H, Plant G, Ghiso J, Frangione B (2000) A decamer duplication in the 3′ region of the BRI gene originates an amyloid peptide that is associated with dementia in a Danish kindred. *Proc Natl Acad Sci USA* **97:** 4920–4925

Weidemann A, Eggert S, Reinhard FB, Vogel M, Paliga K, Baier G, Masters CL, Beyreuther K, Evin G (2002) A novel epsilon-cleavage within the transmembrane domain of the Alzheimer amyloid precursor protein demonstrates homology with Notch processing. *Biochemistry* **41:** 2825–2835

Wilquet V, De Strooper B (2004) Amyloid-beta precursor protein processing in neurodegeneration. *Curr Opin Neurobiol* **14:** 582–588

Wolfe MS (2007) When loss is gain: reduced presenilin proteolytic function leads to increased Abeta42/Abeta40. Talking Point on the role of presenilin mutations in Alzheimer disease. *EMBO Rep* **8:** 136–140

©2011 European Molecular Biology Organization